JOURNAL OF AIRCRAFT
Vol. 39, No. 3, May–June 2002

Automated Method for Transition Prediction on Wings in Transonic Flows

Marc Langlois*
Bombardier Aerospace, Montreal, Quebec H4R 1K2, Canada
Christian Masson†
École de Technologie Supérieure, Montreal, Quebec H3C 1K3, Canada
Fassi Kafyeke‡
Bombardier Aerospace, Montreal, Quebec H4R 1K2, Canada
and
Ion Paraschivoiu§
École Polytechnique de Montreal, Montreal, Quebec H3C 3A7, Canada

The use of stability analyzers based on the linear stability theory and coupled with the e^n method in flowfield calculation procedures (viscous/inviscid interactive methods, Navier–Stokes solvers) has been impeded by that they require tremendous amounts of information, knowledge, and interaction from the user. A systematic procedure is proposed to obtain a linear stability analyzer suitable for integration in wing performance calculation methods. The proposed transition prediction method relies on the use of a database of stability characteristics of a model three-dimensional compressible boundary layer. A coupling method based on the physical parameters of the mean flow, such as local Mach number, Reynolds number, and boundary-layer shape factor, allows the extraction from the database of quantities such as the amplification rate for a given frequency or the maximum amplification frequency of the boundary layer studied. The stability characteristics of the model boundary are precomputed, by the use of the compressible linear stability equations with the classical parallel flow assumption and without curvature effects. The results obtained with the proposed automated stability analysis method have shown that it provides a qualitatively adequate representation of a transonic three-dimensional flow stability characteristics: dominant instability type, frequency of maximum amplification, and amplification rate. Computations of the n factor were performed for the AS409 conical wing and two Bombardier business aircraft wings. For these cases, the automated method n factors are higher than those obtained by a complete eigenvalue calculation. This difference is largely because the model boundary layer used does not provide a completely appropriate representation of the crossflow velocity profiles. However, it is within the range of variation of the n factor from one case to the other, when the full eigenvalue solution is used. Comparison of the calculated n factors and the experimentally observed location of transition on the Bombardier wings has revealed a spanwise variation of the critical n factor, with both the complete and automated calculation methods. To improve the prediction of transition, a relation between the n factor at transition and a local Reynolds number (varying along the span) is proposed. The proposed automated method provides considerable reductions in both the computational time and the input required from the user, which allows it to be incorporated in the design cycle.

Nomenclature

b	=	span, m
c	=	chord, m
c_p	=	specific heat at constant pressure
f	=	dimensional frequency, Hz
$\tilde{f}, g$	=	transformed velocity profiles (similar boundary layer)
H	=	total enthalpy
H_{x_i}	=	streamwise incompressible shape factor
H_{z_i}	=	crossflow incompressible shape factor
i	=	$\sqrt{-1}$
k	=	wave number (wave vector magnitude)
M	=	Mach number
N	=	amplification factor at a fixed frequency
n	=	frequency envelope of N
Pr	=	Prandtl number (0.72)
p	=	pressure
Q	=	total mean velocity
Re	=	Reynolds number
T	=	temperature
t	=	time
t_s	=	similarity parameter
t_w	=	similarity parameter
u, v, w	=	velocity components in x, y, and z
$\boldsymbol{V}_{\mathrm{gr}}$	=	group velocity
$w_{\max}$	=	maximum crossflow velocity
w'_w	=	wall derivative of the crossflow velocity
X, Z, y	=	global coordinate system
x, z, y	=	local Cartesian coordinate system
α	=	complex wave number in the x direction
β	=	complex wave number in the z direction
γ_i	=	total spatial amplification rate
δ_{x_i}	=	streamwise kinematic displacement thickness
δ_{z_i}	=	crossflow kinematic displacement thickness
ε	=	angle between ξ and X

Received 30 April 2001; revision received 17 February 2002; accepted for publication 26 February 2002.

*Engineering Professional, Advanced Aerodynamics. Member AIAA.
†Associate Professor, Mechanical Engineering Department. Member AIAA.
‡Manager, Advanced Aerodynamics. Senior Member AIAA.
§Chair Professor, J.-A. Bombardier Aeronautical Chair, Mechanical Engineering Department. Associate Fellow AIAA.

θ = transformed temperature (enthalpy) profile (similar boundary layer)
θ_{x_i} = streamwise kinematic momentum deficit thickness
θ_{z_i} = crossflow kinematic momentum deficit thickness
Λ = similarity parameter
Λ_{LE} = leading-edge sweep angle
λ = wavelength, or transformed variable (density–viscosity, similar boundary layer)
μ = dynamic viscosity
ξ, η = transformed coordinates (similar boundary layer)
ρ = density
σ = similarity parameter
Φ = arbitrary mean quantity
ϕ = arbitrary instantaneous quantity
$\hat{\phi}$ = amplitude function of the fluctuation of ϕ
χ = similarity parameter
ψ = wave vector orientation with respect to streamline at the boundary-layer edge
ω = complex frequency

Subscripts

e = value at the boundary-layer edge
i = imaginary component
r = real component
w = value at the wall
0 = total (stagnation) value (temperature and enthalpy)
∞ = freestream value

Superscripts

max = value corresponding to the maximum amplification rate at a fixed frequency
opt = value corresponding to the absolute maximum amplification rate

Introduction

FOR many years, environmental and economic issues have been driving research aimed at the reduction of airliners and business aircraft fuel consumption. The latter being tightly related to the drag that must be overcome in flight, one of the promising avenues to this goal lies in reducing friction drag by limiting the extent of turbulent flow over the wings.[1,2] The design of such wings requires a capability to predict accurately the transition from laminar to turbulent flow. In addition, the position of transition on a wing must also be known for the pressure distribution and the drag to be properly predicted, as well as for the extrapolation of wind-tunnel measurements to flight conditions.[3] A reliable and efficient method for predicting the transition point from laminar to turbulent flow thus becomes an invaluable tool to wing-design engineers.

Linear stability theory (LST) is able to provide information about wave amplification and, when coupled to the empirical e^n method, yields insight about the location of boundary-layer transition. A number of LST-based transition prediction codes were conceived during the last 20 years and applied to increasingly complex geometries and flow conditions.[4–6] However, linear stability calculations can be extremely costly in terms of computer and user time, and this has impeded their use in an industrial design context. In addition, they demand knowledge, information, and interaction from the user. The user has to 1) locate and identify the instabilities present in the flow, 2) select the instabilities that are susceptible of triggering transition, and 3) track properly the amplification maxima in the integration of the n factor.

Another issue is the choice of the value of the n factor at transition. Whereas the e^n method was extensively validated for two-dimensional incompressible flows, little experimental data exist concerning transition on realistic wing configurations in compressible transonic flows.

This paper describes an automated database method for the evaluation of the stability characteristics of three-dimensional compressible boundary layers. The main advantage of the method is the significant gains in both computational time and user involvement that it can provide, making its incorporation in the design cycle possible.

LST

The basis of the LST is the decomposition of the instantaneous flow variables into a mean, steady part and a time-dependent perturbation of a sinusoidal form:

$$\phi(x, y, z, t) = \Phi(y) + \hat{\phi}(y) \exp[i(\alpha x + \beta z - \omega t)] \qquad (1)$$

where ϕ represents any of the flow variables, that is, the velocity components u, v, and w in the streamwise x, wall-normal y, and crossflow z directions, the pressure p, and the temperature T. $\Phi(y)$ is the known laminar mean flow, which is assumed to be parallel, whereas α and β are the streamwise and crossflow wave numbers of the perturbation and ω its complex frequency.

After substitution of Eq. (1) into the governing equations, subtraction of the laminar mean flow solution, linearization and other manipulations, a homogeneous system of five, second-order ordinary differential equations is obtained. Given homogeneous boundary conditions, the task then reduces to the resolution of an eigenvalue problem for the determination of the values of the complex parameters α, β, and ω that yield nontrivial solutions.

The eigenvalue problem provides two real relations, but there are six real parameters to be determined. Basic assumptions about the nature of the eigenvalues are, therefore, required. It is customary to specify that one or two of the parameters be pure real numbers. In the case of the temporal stability theory used in the present work, α and β are assumed to be real. One can see then that the real part of ω, that is, ω_r, corresponds to the frequency and its imaginary part ω_i, to the temporal growth rate of the perturbation. Laburthe[7] has shown that except for pathological cases, the use of the temporal formulation together with Gaster's transformation[8] provides amplification rates that are in very good agreement with the results of the more accurate spatial theory. This is confirmed by the experience of the authors in transonic wing applications.

Because the eigenvector $\hat{\phi}$ depends only on y and the mean flow has been assumed parallel, it is possible to apply a local analysis, that is, the determination of the stability characteristics at a given point on a wing involves only the local boundary-layer properties, no information is required from the neighborhood. This essential feature allows precalculated stability characteristics of model boundary layers to be used for the identification and location of the instabilities in the actual boundary layer growing on a wing.

Transition Prediction

Laminar flows are affected by various forced disturbances. If the amplitude of a perturbation is relatively small, its propagation characteristics may be adequately described by the linear stability equations. The ensuing analysis describes the observed exponential growth, or decay, of initially infinitesimal disturbances traveling through the boundary layer. If the amplitude of these waves becomes large enough, nonlinear interactions become important and may lead to transition. Although LST cannot describe nonlinear interactions, there is sufficient empirical evidence suggesting that the process of transition can be correlated to a critical perturbation amplitude ratio. This observation leads to the so-called e^n method in which the n factor is calculated by integrating the spatial growth rate in the direction of the real part of the group velocity γ_i, for a given dimensional frequency f. Different integration strategies arise from that, with fixed f, there still remains the wave numbers α and β to be determined.[9] In this work, the envelope method, in which α and β are determined in such a way as to maximize the spatial growth rate at each position on the wing, is used:

$$N(f, s) = \int_{s_0}^{s} \gamma_i^{\max}(f, s)\, \mathrm{d}s \qquad (2)$$

where

$$\gamma_i^{\max}(f, s) = \max_{\alpha,\beta} \{\gamma_i(f, \alpha, \beta, s)\}$$

and the integration path s is tangent to the amplification vector. The spatial growth rate γ_i is obtained from the temporal growth rate ω_i, using Gaster's relation[8]:

$$\gamma_i = \omega_i / |\boldsymbol{V}_{\mathrm{gr}}| \tag{3}$$

where $\boldsymbol{V}_{\mathrm{gr}}$ is the real part of the group velocity. Finally, the n factor used for transition prediction is obtained by taking the envelope of N for all frequencies:

$$n(s) = \max_f N(f, s) \tag{4}$$

As already mentioned, other strategies for the integration of the n factor exist. Some researchers argue that methods that allow a clearer distinction between crossflow and streamwise instabilities are preferable to the envelope method (for instance, Ref. 10). However, in terms of the ability of one method to better and more consistently predict transition than an other, a clear advantage has yet to be demonstrated.[9] It is also known that the envelope method may fail when boundary-layer suction is employed (hybrid laminar flow), but we are only concerned here with natural laminar flow applications.

Automated Stability Calculations Methodology

The location and identification of the instabilities present on a wing, that is, the determination of their neutral point, as well as their orientation and wavelength, are conducted with the use of known tabulated stability solutions of a model (self-similar) boundary layer. Schemes for the rapid evaluation of the stability characteristics of two-dimensional incompressible flows have been proposed by Stock and Degenhart,[11] Dini et al.,[12] and Gaster and Jiang,[13] among others. These methods assume that the velocity profiles on an airfoil can be well represented by the Falkner–Skan family of self-similar profiles (the method of Dini et al.[12] also uses modified Green profiles for separated flows). A matching procedure is used to evaluate the stability characteristics of the actual (nonsimilar) boundary-layer profiles of interest from those of the model boundary-layer profiles. The calculation of n factors is conducted directly from the model boundary-layer stability characteristics. The Arnal–Vialle–Jelliti criterion for transition due to streamwise instability (see Ref. 14) (also known as the parabola method) is another example of such a fast n-factor method. The proposed methodology is an extension of the two-dimensional incompressible matching method of Gaster and Jiang[13] to three-dimensional compressible flows. Such a method relies on the local nature of the eigenvalue problem in the linear parallel stability theory. It implies, however, that the main nonparallel effects cannot be taken into account. Surface curvature effects could theoretically be included, but at the expense of a considerable increase in the size of the database. Furthermore, if curvature is to be included, other second-order effects such as nonlocality must also be included to obtain a consistent stability model. Based on previous investigations, however, it was concluded that neither the curvature effects nor the nonparallel effects significantly improve the consistency of the n factor at transition.[15,16] With regard to the curvature effects, similar conclusions were also reached by Cebeci et al.[17] for incompressible flows. Therefore, it is legitimate to neglect these effects in a transition prediction method.

Model Boundary Layer

To construct the database of stability characteristics, it is necessary to have available a family of boundary-layer profiles describing the flow on a three-dimensional wing in compressible flow. In the present work, a one-species variant of the model proposed by Dewey and Gross[18] has been selected. This model provides a family of compressible boundary layers on an infinite swept wing and is essentially a compressible extension of the Falkner–Skan–Cooke family of similar boundary-layer profiles. Figure 1 represents the flow under consideration and the coordinate systems used.

A global (X, Z, y) and a local (x, z, y) coordinate system are used, where y is normal to the surface and X and Z (x and z) are tangent to it. In the global system X is normal to the leading edge,

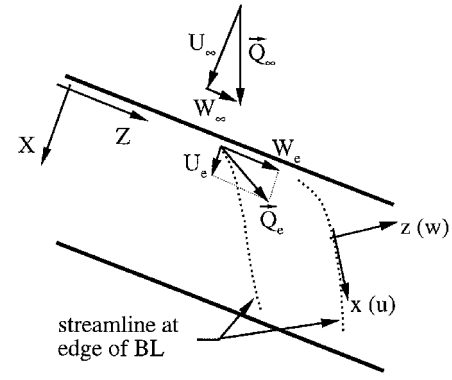

Fig. 1 Infinite swept wing flow.

whereas in the local system, x is in the direction of the inviscid streamline at the edge of the boundary layer. The x-momentum, z-momentum, and energy equations of the proposed model boundary layer are, respectively,

$$(\lambda \tilde{f}'')' + \tilde{f}\tilde{f}'' = \Lambda\left\{\tilde{f}'^2 - (1/t_s)\left[(1-t_w)\theta - (1-t_s)g^2 + t_w\right]\right\} \tag{5}$$

$$(\lambda g')' + \tilde{f}g' = 0 \tag{6}$$

$$(\lambda\theta')' + Prf\theta' = 2[(1-Pr)/(1-t_w)]\{\lambda[\chi(\sigma + t_s - 1)\tilde{f}'\tilde{f}'' + (1-t_s)gg']\}' \tag{7}$$

The velocity U and W and temperature T (or enthalpy H) profiles are defined by

$$\tilde{f}' = \tilde{f}'(\eta) = U/U_e, \qquad g = g(\eta) = W/W_e$$

$$\theta = \theta(\eta) = (H - H_w)/(H - H_e)$$

$$H = H(\eta) = c_pT + (U^2 + W^2)/2$$

$$\lambda = \lambda(\eta) = \rho\mu/\rho_w\mu_w = T_w\mu/T\mu_w$$

A prime ($'$) denotes differentiation with respect to η, the normal-to-the-wall coordinate. Subscripts w and e represent quantities at the wall and at the boundary-layer edge, respectively. The independent coordinates x and y have been transformed to

$$\xi(X) = \int_0^X \rho_w\mu_w U_e \,\mathrm{d}X, \qquad \eta(X, y) = \frac{U_e}{\sqrt{2\xi}}\int_0^y \rho \,\mathrm{d}y$$

Assuming an adiabatic wall, the boundary conditions, at the wall are

$$\tilde{f}(0) = \tilde{f}'(0) = g(0) = \theta'(0) = 0$$

and at the edge are

$$\tilde{f}'(\eta_e) = g(\eta_e) = \theta(\eta_e) = 1$$

The external flow is assumed isentropic, and, therefore,

$$H_e = \text{const} = H_0 = c_pT_0$$

with T_0 the stagnation temperature.

The similarity parameters are

$$\chi = \left(\frac{u_e}{u_\infty}\right)^2 \tag{8}$$

$$\sigma = \frac{U_\infty^2}{2H_e} = \frac{U_\infty^2}{2c_pT_0} \tag{9}$$

$$t_s = 1 - \sigma \sin^2 \Lambda_{\mathrm{LE}} \tag{10}$$

$$\Lambda = \frac{2\xi}{U_e}\frac{\mathrm{d}U_e}{\mathrm{d}\xi}\frac{T_0}{T_e}t_s \tag{11}$$

$$t_w = \frac{H_w}{H_e} = \frac{T_w}{T_0} \tag{12}$$

Note that for an incompressible flow ($\sigma = 0$) with constant density and viscosity, Eqs. (5) and (6) reduce to the Falkner–Skan–Cooke equations.

Matching Procedure

Physical quantities of interest can be obtained from the preceding definitions of the five similarity parameters:

$$M_\infty^2 = \frac{2\sigma}{(\gamma-1)(1-\sigma)} \tag{13}$$

$$U_e^2 = 2c_pT_0(\sigma + t_s - 1)\chi \tag{14}$$

$$W_e^2 = 2c_pT_0(1 - t_s) \tag{15}$$

$$T_e = T_0[t_s - (\sigma + t_s - 1)\chi] \tag{16}$$

$$M_e^2 = \frac{2}{\gamma-1}\frac{1 - t_s + (\sigma + t_s - 1)\chi}{t_s - (\sigma + t_s - 1)\chi} \tag{17}$$

where M_∞ and M_e are the Mach numbers related to the freestream velocity Q_∞ and $Q_e[=\sqrt{(U_e^2 + W_e^2)}]$, respectively. Because U_e^2, W_e^2, and T_e must all be positive, Eqs. (14–16) imply the following restrictions on the similarity parameters:

$$t_s < 1, \qquad (\sigma + t_s - 1)\chi > 0, \qquad t_s - (\sigma + t_s - 1)\chi > 0$$

For the matching with the actual boundary layer growing on a wing and the calculation of the stability characteristics, the local coordinate system defined earlier (x, z, y) is used. The velocity profiles in this system are

$$\frac{u}{Q_e} = \frac{(\sigma + t_s - 1)\tilde{f}' + (1 - t_s)g}{(\sigma + t_s - 1)\chi + 1 - t_s} \tag{18}$$

$$\frac{w}{Q_e} = \frac{(1 - t_s)(\sigma + t_s - 1)\chi}{(\sigma + t_s - 1)\chi + 1 - t_s}(g - \tilde{f}') \tag{19}$$

The temperature profiles are expressed as

$$\frac{T}{T_e} = \frac{(\theta - 1)\left[(\sigma + t_s - 1)\chi\,\tilde{f}'^2 + (1 - t_s)g^2\right]}{(\theta - 1)[t_s - (\sigma + t_s - 1)\chi]} \tag{20}$$

Matching procedures typically use the incompressible shape factors in the streamwise and crossflow directions, defined as

$$H_{x_i} = \delta^*_{x_i}\big/\theta_{x_i} \tag{21}$$

$$H_{z_i} = \delta^*_{z_i}\big/\theta_{z_i} \tag{22}$$

where

$$\delta^*_{x_i} = \int_0^\infty \left(1 - \frac{u}{Q_e}\right)\mathrm{d}\eta, \qquad \delta^*_{z_i} = \int_0^\infty -\frac{w}{Q_e}\,\mathrm{d}\eta$$

$$\theta_{x_i} = \int_0^\infty \frac{u}{Q_e}\left(1 - \frac{u}{Q_e}\right)\mathrm{d}\eta, \qquad \theta_{z_i} = \int_0^\infty -\left(\frac{w}{Q_e}\right)^2\mathrm{d}\eta$$

As mentioned earlier, there are five nondimensional parameters that specify a given self-similar boundary layer: σ, t_s, t_w, Λ, and χ. The aim of the matching procedure is to determine the combination of these parameters that will produce a model boundary layer having stability characteristics similar to those of the actual boundary layer of interest. In this work, only adiabatic-wall boundary layers are considered. In this case, there is only one possible value of t_w for a given combination of the other parameters. The σ and χ parameters can be obtained directly from the flow conditions of the physical boundary layer, by inverting Eqs. (13) and (17)

$$\sigma = \frac{[(\gamma-1)/2]M_\infty^2}{1 + [(\gamma-1)/2]M_\infty^2} \tag{23}$$

$$\chi = \frac{\left\{1 + [(\gamma-1)/2]M_e^2\right\}t_s - 1}{(\sigma + t_s - 1)\left\{1 + [(\gamma-1)/2]M_e^2\right\}} \tag{24}$$

For the determination of the remaining two parameters, t_s and Λ, it is necessary to require that some measurable properties of the model boundary layer be as close as possible to the same properties measured on the actual boundary layer on the wing. Note that Eq. (10) is not used to determine t_s directly because we are considering boundary layers growing on an arbitrary wing (not an infinite swept wing). Following the approach taken in two-dimensional incompressible flows,[13] the incompressible shape factor in the local streamwise direction, H_{x_i}, is used. This should ensure closeness of the streamwise velocity profiles (u/Q_e). By extension, the second property may be chosen to be the incompressible shape factor in the crossflow direction, H_{z_i}. This is one of the options that were considered, together with the maximum crossflow velocity and the nondimensional crossflow-velocity derivative at the wall. The latter quantities are defined as

$$w_{\max} = \max_\eta \left|\frac{w}{Q_e}\right| \tag{25}$$

$$w'_w = \frac{\delta_{x_i}}{Q_e}\frac{\mathrm{d}w}{\mathrm{d}\eta}\bigg|_w \tag{26}$$

It was found[19] that the streamwise incompressible shape factor H_{x_i} provides a very good representation of the streamwise velocity profile, even in strongly decelerated flows. It has also been observed that the value of the pressure-gradient parameter Λ is almost uniquely determined by this shape factor. The matching of the crossflow velocity profile is less straightforward. The distance of the crossflow velocity maximum from the surface and the presence of multiple crossflow velocity maxima (S-shaped profiles) are features that have a significant influence on the stability characteristics. One of the most important limitations of the Dewey and Gross[18] model is actually its inability to predict S-shaped crossflow velocity profiles. Therefore, it was important to base the choice of the matching criteria not so much on the reproduction of the boundary layer profiles but on the overall agreement of the stability characteristics. In accelerated flows ($\Lambda > 0$), where the importance of the crossflow velocity profile is greatest, the $w_{\max}$ criterion seems to produce the best agreement of velocity profiles and stability characteristics, with the H_{z_i} criterion being almost equally good. In decelerated flows ($\Lambda < 0$), the w'_w matching and the $w_{\max}$ criterion provide a better representation of the streamwise instabilities than the H_{z_i} criterion. Based on these observations, the $w_{\max}$ criterion has been retained as the crossflow matching parameter.

Database of Stability Characteristics

A systematic procedure was developed to investigate the stability characteristics of three-dimensional transonic flows and to predict transition.[20] The application of this procedure to a number of test cases has highlighted the main requirements of an automated transition prediction method, which are 1) to identify the nature of the dominant instability, 2) to evaluate the critical frequency range, 3) to locate the neutral points of instabilities, and 4) to evaluate the n factor.

To achieve these objectives, the following information is required: 1) the wave number k^{opt} $[k = \sqrt{(\alpha^2 + \beta^2)}]$ and orientation ψ^{opt} (defined with respect to the inviscid streamline) of the most amplified disturbance and 2) the spectral distribution of the maximum amplification rate $\gamma_i^{\max}(\omega_r)$.

For a given value of the freestream temperature T_∞, and in the framework of the chosen model boundary layer over an adiabatic wall, these stability characteristics are functions of the four similarity parameters σ, χ, Λ, and t_s and of the Reynolds number Re_δ of interest. This Reynolds number is based on the local streamwise velocity Q_e and displacement thickness $\delta^*_{x_i}$. As discussed in the preceding section, these four similarity parameters can be matched with the following, more physically relevant, parameters: Mach number M_∞, Mach number M_e, H_{x_i} and $w_{\max}$. Symbolically, the functionality of the stability characteristics k^{opt}, ψ^{opt}, and $\gamma_i^{\max}$ with respect to the independent parameters can be written as

$$k^{\text{opt}}\left(M_\infty, M_e, H_{x_i}, w_{\max}, Re_\delta\right), \qquad \psi^{\text{opt}}\left(M_\infty, M_e, H_{x_i}, w_{\max}, Re_\delta\right)$$

$$\gamma_i^{\max}\left(\omega_r, M_\infty, M_e, H_{x_i}, w_{\max}, Re_\delta\right)$$

To reduce the size of the database, the spectral distribution of $\gamma_i^{\max}$ is approximated as a cubic function of ω_r:

$$\gamma_i^{\max}(\omega_r) = a\omega_r^3 + b\omega_r^2 + c\omega_r + d \tag{27}$$

The maximum amplification frequency ω_r^{opt} can easily be obtained from the preceding relation as

$$\omega_r^{\text{opt}} = \omega_r \qquad \text{when} \qquad \frac{\mathrm{d}\gamma_i^{\max}}{\mathrm{d}\omega_r} = 0$$

$$= \frac{-b \pm \sqrt{b^2 - 3ac}}{3a} \tag{28a}$$

such that

$$\left.\frac{\mathrm{d}^2\gamma_i^{\max}}{\mathrm{d}\omega_r^2}\right|_{\omega_r^{\text{opt}}} = 6a\omega_r^{\text{opt}} + 2b < 0 \tag{28b}$$

from which the maximum amplification rate is then obtained.

The database of stability characteristics is simply a table of k^{opt}, ψ^{opt}, and $\gamma_i^{\max}$ (represented by the coefficients a, b, c, and d) for a number of discrete values of the independent parameters Mach number M_∞, Mach number M_e, H_{x_i}, $w_{\max}$, and Reynolds number Re_δ. It can be represented in the following compact form:

$$k^{\text{opt}}\left(M_\infty, M_e, H_{x_i}, w_{\max}, Re_\delta\right) \tag{29}$$

$$\psi^{\text{opt}}\left(M_\infty, M_e, H_{x_i}, w_{\max}, Re_\delta\right) \tag{30}$$

$$a\left(M_\infty, M_e, H_{x_i}, w_{\max}, Re_\delta\right) \tag{31}$$

$$b\left(M_\infty, M_e, H_{x_i}, w_{\max}, Re_\delta\right) \tag{32}$$

$$c\left(M_\infty, M_e, H_{x_i}, w_{\max}, Re_\delta\right) \tag{33}$$

$$d\left(M_\infty, M_e, H_{x_i}, w_{\max}, Re_\delta\right) \tag{34}$$

The parameter t_w does not appear in Eqs. (29–34) because the database is restricted to boundary layers over adiabatic walls. The freestream temperature T_∞ should also appear in Eqs. (29–34) because it influences the nondimensional viscosity profile calculated through Sutherland's relation. However, to reduce the number of independent parameters, it has been decided to construct the database for a given value of T_∞. This is not a severe limitation because transition predictions typically involve only two freestream temperatures, namely, that observed at the aircraft cruising altitude and that occurring in a wind tunnel. This means that different databases should be constructed for transition predictions in-flight and in a wind tunnel. The original implementation of the database method corresponds to flight conditions with $T_\infty = 215$ K.

The database structure and the matching procedure were validated by conducting calculations on the ONERA M6 and NASA Ames Research Center wings.[21,22] This validation exercise has also provided an identification of the ranges of values for the matching parameters. Based on this and the typical flight conditions of interest, the following ranges were selected:

$$0.7 \le M_\infty \le 0.9, \qquad 0.2 \le M_e \le 2.0, \qquad 2.0 \le H_{x_i} \le 3.0$$

$$0 \le w_{\max} \le 0.25, \qquad 500 \le Re_\delta \le 10{,}000 \tag{35}$$

Results

Transition prediction results using the database method will be presented first on the simple conical AS409 wing, then on two realistic Bombardier wings with spanwise pressure gradients. The viscous mean flow was calculated using the fully three-dimensional procedure described in Ref. 20, which combines a three-dimensional Euler solver and a three-dimensional compressible boundary-layer code.

AS409 Conical Wing

This test case was used to investigate how well the database method reproduces the evolution of the stability characteristics predicted by the complete LST computations. Results will be presented for test 42 of Ref. 23, for which the freestream Mach and Reynolds numbers were 0.74 and 12.8×10^6, respectively. The freestream temperature was 131 K, which differs from that used in the construction of the database (215 K). Also, only one freestream Mach number value, 0.85, had been incorporated in the database at the time these computations were conducted. Thus, it was decided to verify the influence of these deviations on the stability characteristics. For identical values of $M_\infty = 0.85$, $M_e = 1.0$, $Re_\delta = 3.5 \times 10^3$, $H_{x_i} = 2.53$, and $w_{\max} = 0.0093$, the boundary-layer profiles were first compared for T_∞ values of 215 and 131 K. With $T_\infty = 215$ K, the same comparisons were made when Mach number M_∞ is varied. The velocity and temperature profiles are identical in all cases; however, the values of T_e are different, which implies that the viscosity profiles will be different. Stability calculations were then conducted, and Table 1 shows that the influence of T_∞ and Mach number M_∞ on the optimum wave amplification and frequency is negligible, which indicates that the database can be used even though the values of these parameters in the present case are different from the nominal ones.

The results of the most unstable wave tracking are presented in Figs. 2–5. The wavelength and orientation of the most unstable wave are shown in Figs. 2 and 3. The complete LST results indicate

Table 1 AS409 wing: validation

T_∞	M_∞	T_e	ω_i^{opt}	ω_r^{opt}
215	0.85	205	1.74×10^{-3}	4.45×10^{-2}
131	0.85	125	1.79×10^{-3}	4.49×10^{-2}
215	0.74	199	1.74×10^{-3}	4.45×10^{-2}

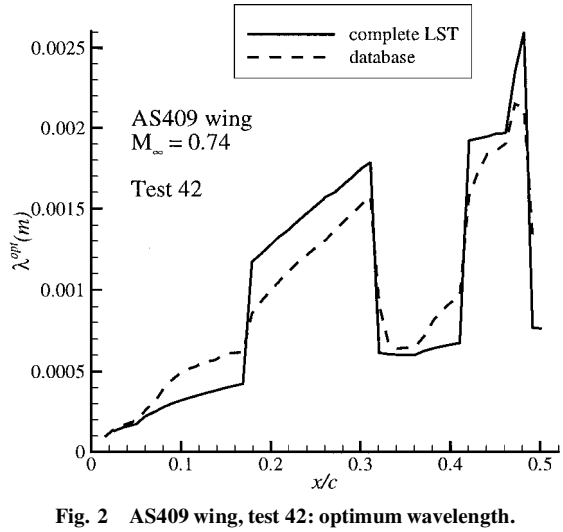

Fig. 2 AS409 wing, test 42: optimum wavelength.

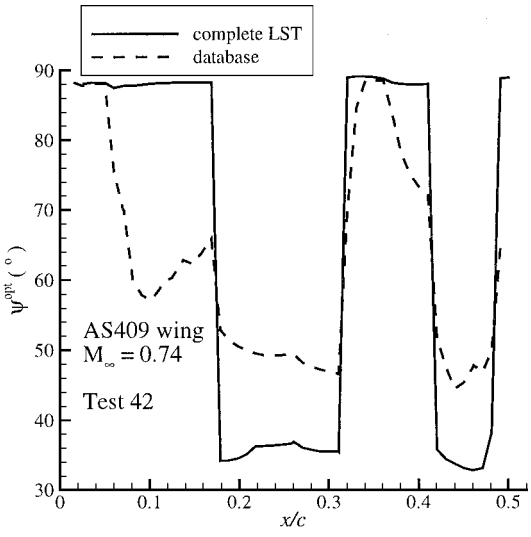

Fig. 3 AS409 wing, test 42: optimum wave orientation.

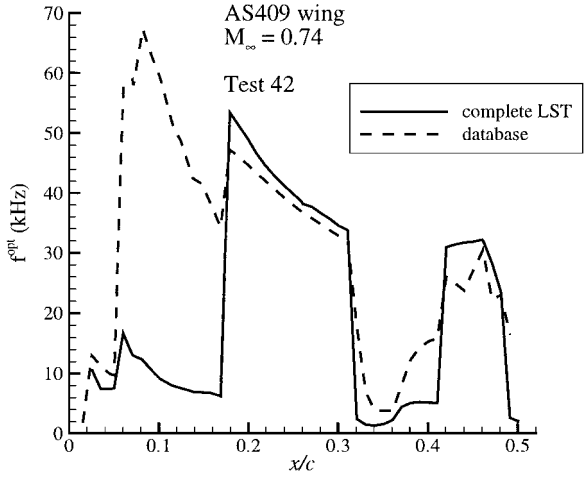

Fig. 4 AS409 wing, test 42: optimum frequency.

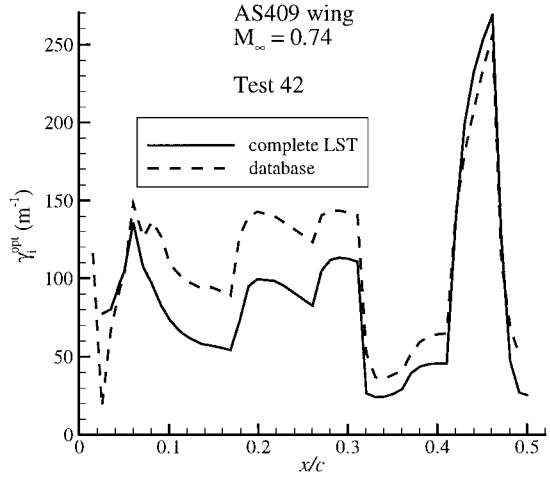

Fig. 5 AS409 wing, test 42: optimum growth rate.

a later evolution from a crossflow to a streamwise instability than the database predictions. The subsequent changes of dominant instability type are well predicted, even though the orientations themselves are different. The complete LST method actually predicts a brutal transition from a pure crossflow to a pure streamwise instability, whereas the database method tends to predict instabilities of a mixed nature. The evolution of the optimum wavelength is qualitatively well predicted.

Figure 4 shows the evolution of the maximum amplification frequency. The agreement between the complete and database results is generally good, except in the region where the complete calculations predict a crossflow instability (thus, a low frequency), whereas the database method indicates that a streamwise wave is dominant (corresponding to a high frequency). The evolution of the optimum amplification rate (Fig. 5) is qualitatively well predicted, albeit with levels generally above those from the exact LST solution.

Earlier results[24] have indicated that the critical frequency for test 42 is 20 kHz. Figure 6 presents the chordwise variation of the maximum amplification rate for this frequency. Again, the database results reproduce qualitatively the behavior of the exact solution, even though the actual rates of amplification may be under- or overestimated. The corresponding n factors are shown in Fig. 7. At the experimental transition position, the difference between the two solutions is approximately 0.6. One of the advantages of the database method is that it allows the simultaneous and rapid computation of the n factors for a large range of frequencies. Figure 8 presents the results obtained for frequencies ranging from 0 to 30 kHz, which completely define the envelope. The maximum n factor at the transition location is produced by the 25-kHz instability. The difference between the n factor and that produced by the complete LST at 20 kHz is less than 1, which is actually less than the uncertainty margin of the e^n method for three-dimensional compressible flows.[25]

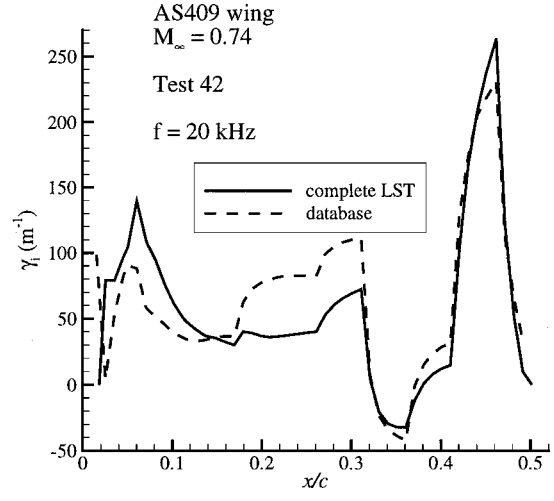

Fig. 6 AS409 wing, test 42: maximum growth rate, $f = 20$ kHz.

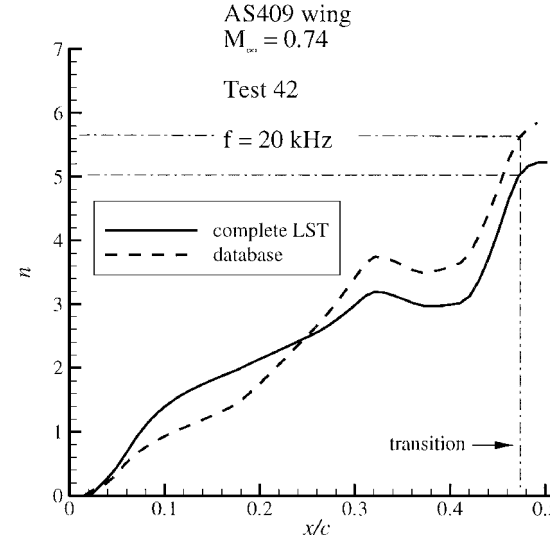

Fig. 7 AS409 wing, test 42: n factor, $f = 20$ kHz.

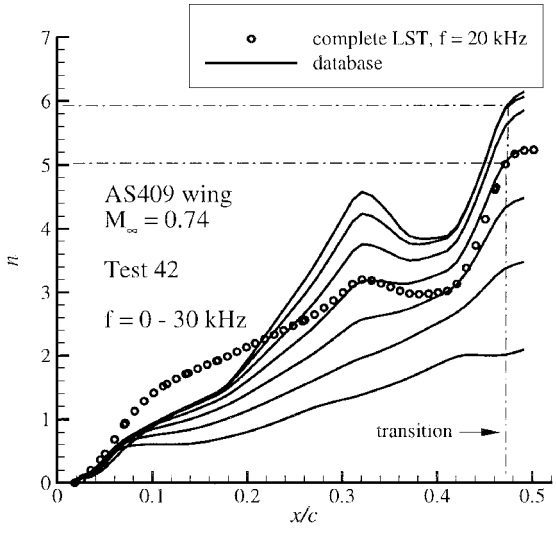

Fig. 8 AS409 wing, test 42: *n* factor, *f* = 0–30 kHz.

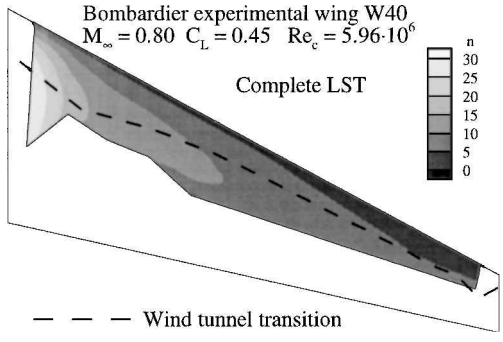

Fig. 9 Bombardier experimental wing W40: upper surface *n* factor, complete LST solution (Bombardier Inc., proprietary data).

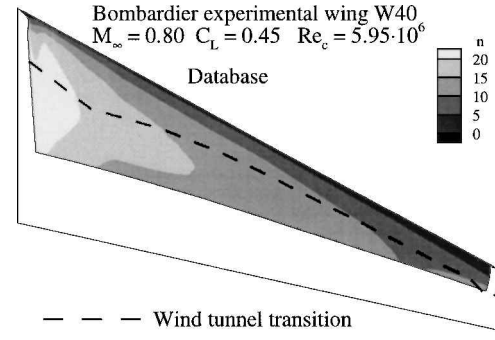

Fig. 10 Bombardier experimental wing W40: upper surface *n* factor, database method (Bombardier Inc., proprietary data).

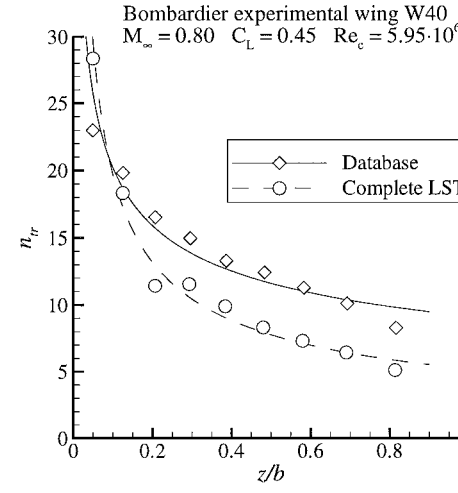

Fig. 11 Bombardier experimental wing W40: transition *n* factor (Bombardier Inc., proprietary data).

Comparisons of Predictions with Three-Dimensional Wind-Tunnel Results

Recent wind-tunnel tests on Bombardier wings have allowed the position transition to be experimentally evaluated. These data provide a comparison basis for the evaluation of different aspects of the transition prediction methods presented earlier.

Bombardier Experimental Wing W40

The first series of results was obtained on a Bombardier-designed experimental wing W40. This wing has a relatively simple planform, with constant moderate leading- and trailing-edge sweep angles. The tests took place in the MicroCraft wind tunnel in California. The flow conditions considered are $M_\infty = 0.80$ (cruise speed), $Re_c = 5.95 \times 10^6$, and $C_L = 0.45$. Note that the experimental results were obtained on a full aircraft configuration (wing, fuselage, empennage, and engines), whereas the boundary-layer computations were performed on an isolated wing. This means the results near the wing root may not be perfectly realistic. This limitation is related to the boundary-layer code used, not to the stability analysis and transition prediction method.

Figures 9 and 10 present the n factor contours on the upper surface of the wing, as predicted by the full LST computation and the database method, respectively. Figures 9 and 10 represent the envelope of the results obtained for many frequencies within the critical range. The experimental position of transition is also shown. The latter was obtained by visualization of the oil flow on the surface of the wing. The isolines of n produced by the two methods present a similar behavior, notably an aft movement from root to tip; however, the levels are different. Except near the wing root, the database method produces higher n factors than the full LST computations. This had already been observed on the AS409 wing. The spanwise variation of the transition n factor is presented in Fig. 11. Two comments can be made. First, except near the wing root ($z/b \leq 0.15$), the critical n factor predicted by the database method is higher than that predicted by the complete calculations, with a nearly constant difference of 4. This could be attributed to the difficulty of the Dewey and Gross[18] model to reproduce the crossflow velocity profiles, as already mentioned. Second, irrespective of the method used, the spanwise variation of the critical n factor is very significant; the difference between n_{tr} at the wing root and n_{tr} at the wing tip is in fact more important than that between the two solutions. Note that two computer runs are required to obtain the N factor curve for each frequency with the complete LST method, the first one starting near the leading edge to catch the crossflow instabilities and the second one farther downstream to get the streamwise instabilities. The location where the nature of the dominant instability changes also needs to be identified. The database method, on the other hand, automatically predicts the passage from a crossflow to a streamwise instability in a single computer run, as shown in Fig. 12. The computing times for a single frequency on a CRAY J932 supercomputer are 57 min for the full LST calculations and 32 s for the database method, and a dozen frequencies are required to define properly the n factor envelope. This certainly demonstrated the usefulness of the database method in an industrial context.

Bombardier BD-700 Global Express Wing

Transition visualizations were also performed on the wing of the ultra-long-range Bombardier Global Express business aircraft, in the National Aerospace Laboratory High Speed Tunnel wind tunnel, in Amsterdam. The fluid used in this case was acenaphtene, and transition determination was done, as in the previous case, approximatively from photographs. However, the position of the cameras for this case was such that a planview could not be obtained, lowering the precision with which the transition position could be determined.

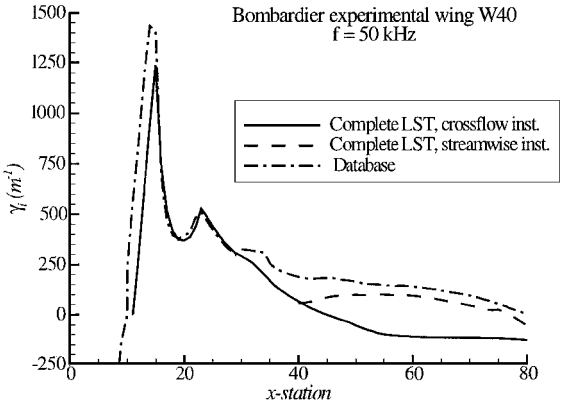

Fig. 12 Bombardier experimental wing W40: amplification rate, $f = 50$ kHz (Bombardier Inc., proprietary data).

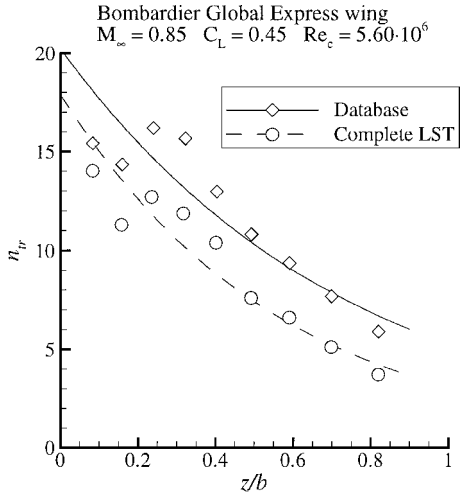

Fig. 13 Bombardier Global Express wing at $Re = 5.6 \times 10^6$: transition n factor (Bombardier Inc., proprietary data).

The Mach number and lift coefficient for these tests were respectively 0.85 and 0.45 (cruise condition). Results were obtained for two Reynolds number values, $Re_c = 5.60 \times 10^6$ and 3.20×10^6.

Figure 13 shows the spanwise variation of the transition n factor for the high Reynolds number test. As with wing W40, both methods predict a significant spanwise decrease of the critical n factor and a nearly constant difference between the two solutions. Similar results were obtained for the low Reynolds number case.

Critical n-Factor Determination

The preceding results indicate that it is not possible to establish a single value of the transition n factor for the configurations considered. The observed variation of the critical n factor can be linked, at least in part, to the relative strength of the streamwise and crossflow instabilities: according to transition measurements made in flight on the VFW-614 and Fokker 100 (Refs. 10 and 25), the critical n factor is higher when transition is mainly affected by crossflow instabilities than when it is caused by streamwise instabilities. From a transition prediction standpoint, it is needed to relate the critical n factor to the mean flow parameters. The results presented in the preceding sections and shown again in Figs. 14 and 15 lead us to the assumption that a proper correlation parameter should have the form of a local-chord c' Reynolds number, to represent the spanwise variation of n_{tr}. The leading edge sweep angle Λ_{LE} (also spanwise variable) should also be involved because it significantly influences the nature of the dominant instability. The proposed correlation parameter is, therefore, defined as

$$Re_{c'U} = Q_\infty c' \cos \Lambda_{LE} / \nu_\infty \tag{36}$$

The variation of the transition n factor with this parameter has been plotted in Figs. 16 (complete LST) and 17 (database method). The

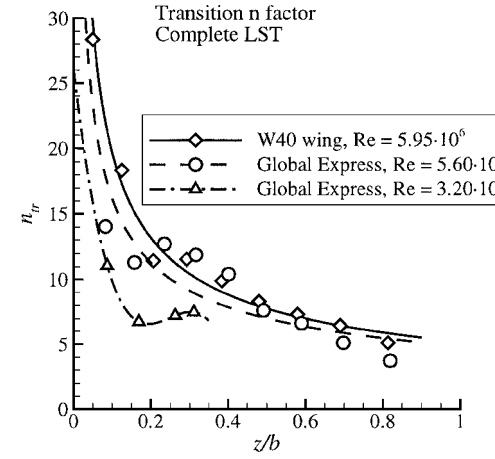

Fig. 14 Transition n factor: complete LST solution (Bombardier Inc., proprietary data).

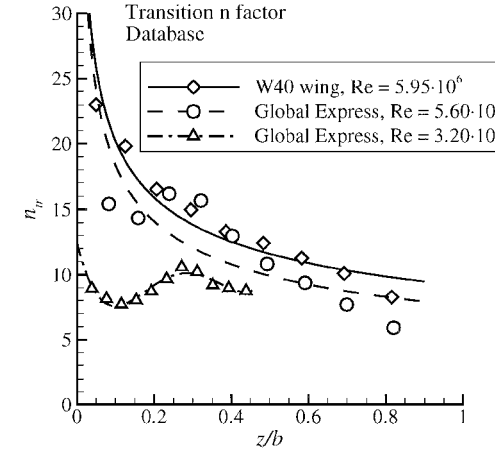

Fig. 15 Transition n factor: database method (Bombardier Inc., proprietary data).

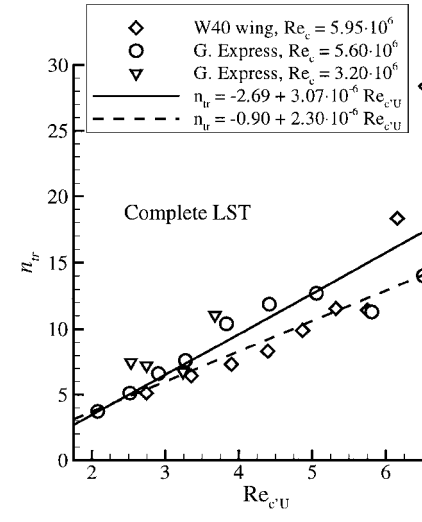

Fig. 16 Transition n factor: correlation with Reynolds number $Re_{c'U}$, complete LST solution (Bombardier Inc., proprietary data).

least-square linear fits through the data are also presented. The solid lines represent the correlations obtained when all data points are included. Removing the point at the highest Reynolds number produces the correlations illustrated in dashed lines. This point corresponds to the spanwise section closest to the wing root on wing W40, where the boundary-layer solution may not be fully reliable due to the absence of the fuselage. Removing this point significantly improves the standard deviation of the correlations. Higher-order

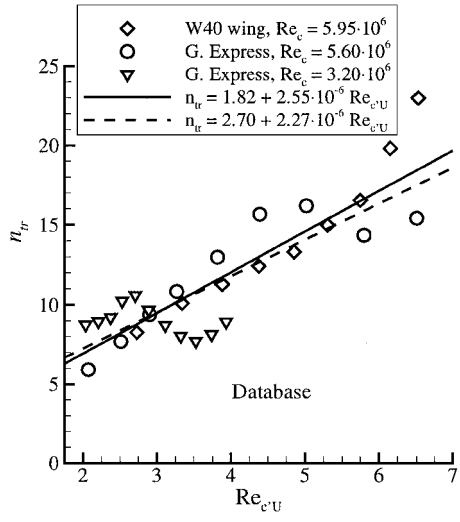

Fig. 17 Transition n factor: correlation with Reynolds number $Re_{c'U}$, database method (Bombardier Inc., proprietary data).

correlations do not provide any significant improvement over the linear fits. The database method, together with the critical n factor determined by the correlation

$$n_{\text{tr}} = 2.70 + 2.27 \times 10^{-6} Re_{c'U} \tag{37}$$

has been used successfully at Bombardier for the prediction of transition in subsequent wind-tunnel tests. Whereas it is recognized that the preceding correlation is in no way universal, it can provide a reliable indication of transition location in conditions similar to those presented in this paper. Different values of the critical n factor could be expected, for instance, in flight conditions where the freestream turbulence levels are much lower than in wind tunnels.

Conclusions

This paper presented an automated database method for the evaluation of stability characteristics and the prediction of laminar/turbulent transition in three-dimensional compressible flows. The method is fast and relatively easy to use, making it appropriate for use in an industrial context. It relies on a database of stability characteristics built from a compressible three-dimensional model boundary layer. The results of the complete LST eigenvalue solution and the proposed method were compared for the AS409 wing. This has indicated that the database method correctly predicts the overall evolution of the stability characteristics, even though differences exist in absolute values.

The database method was then used to calculate the n factor on the Bombardier Global Express wing and the experimental wing W40. The predicted n factors were correlated with the position of transition observed in wind-tunnel tests. This has revealed a spanwise variation of the critical n factor that is also observed when the full LST equations are solved, meaning that a single value of the n factor can not be used as a transition criterion. Instead, a correlation of the critical n factor with a local-chord-based Reynolds number is proposed. This criterion is now used with the database method for transition prediction on Bombardier aircraft wings before wind-tunnel tests. Further validations are required to establish whether the correlation is also valid for transition in flight. As a next step, the database method should be implemented directly in Bombardier's Euler/boundary-layer and Navier–Stokes solvers.

Acknowledgments

This work was supported in part by the Natural Sciences and Engineering Research Council of Canada, through a Collaborative Research and Development Grant with Bombardier Aerospace. The first author would also like to acknowledge the assistance provided by the Fonds pour la Formation de Chercheurs et l'Aide à la Recherche, Government of Québec, in the form of postgraduate scholarships.

References

[1]Cousteix, J., and Schmitt, V., "Réduction de la traînée aérodynamique," *Nouvelle revue d'aéronautique et d'astronautique*, No. 1997-1, 1997, pp. 34–41.

[2]Kingsley-Jones, M., "Airbus Plans Laminar Flow Tests in Bid to Bring Down Fuel Costs," *Flight International Magazine*, Vol. 153, No. 4627, 1998, p. 41.

[3]Elsenaar, A., and Haines, A. B., "Empirical Tools for Simulations Methodologies," AGARD AR-224, 1988, pp. 132–138.

[4]Malik, M. R., and Orszag, S. A., "Efficient Computation of the Stability of Three-Dimensional Compressible Boundary Layers," AIAA Paper 81-1277, 1981.

[5]Cebeci, T., and Chen, H. H., "Numerical Method for Predicting Transition in Three-Dimensional Flows by Spatial Amplification Theory," *AIAA Journal*, Vol. 30, No. 8, 1992, pp. 1972–1979.

[6]Arnal, D., Habiballah, M., and Coustols, E., "Théorie de l'instabilité laminaire et critères de transition en écoulement bi et tridimensionnel," *La Recherche Aérospatiale*, No. 1984-2, 1984, pp. 125–143.

[7]Laburthe, F., "Problème de stabilité linéaire et prévision de la transition dans des configurations tridimensionnelles, incompressibles et compressibles," Ph.D. Dissertation, École Nationale Supérieure de l'aéronautique et de l'espace, Toulouse, Dec. 1992.

[8]Gaster, M., "A Note on a Relation Between Temporally Increasing and Spatially Increasing Disturbances in Hydrodynamic Stability," *Journal of Fluid Mechanics*, Vol. 14, 1962, pp. 222–224.

[9]Arnal, D., "Boundary Layer Transition: Predictions Based on Linear Theory," AGARD R-793, Progress in Transition Modelling, 1993, pp. 2.1–6.

[10]Schrauf, G., "Transition Prediction Using Different Linear Stability Analysis Strategies," *Proceedings of the AIAA 12th Applied Aerodynamics Conference*, AIAA, Washington, DC, 1994, pp. 367–375.

[11]Stock, H. W., and Degenhart, E., "A Simplified e^n Method for Transition Prediction in Two-Dimensional, Incompressible Boundary Layers," *Zeitschrift für Flugwiss. Weltraumforsch.*, Vol. 13, 1989, pp. 16–30.

[12]Dini, P., Selig, M. S., and Maughmer, M. D., "Simplified Linear Stability Transition Prediction Method for Separated Boundary Layers," *AIAA Journal*, Vol. 30, No. 8, 1992, pp. 1953–1961.

[13]Gaster, M., and Jiang, F., "A Rapid Scheme for Estimating Transition on Wings by Linear Stability Theory," *ICAS Proceedings 1994 19th Congress of the International Council of the Aeronautical Sciences*, 1994, pp. 1104–1113.

[14]Arnal, D., "Transition Prediction in Transonic Flow," *Symposium Transsonicum III, IUTAM Symposium*, Springer-Verlag, Berlin, Heidelberg, 1989, pp. 253–262.

[15]Langlois, M., Masson, C., Paraschivoiu, I., and Tezok, F., "Curvature Effects in 3-D Compressible Transition Analysis," *Proceedings of the Third Annual Conference of the CFD Society of Canada*, Distributed by National Research Council Canada, Ottawa, 1995, pp. 315–322.

[16]Langlois, M., Casalis, G., and Arnal, D., "On the Practical Application of the PSE Approach to Linear Stability Analysis," *Aerospace Science and Technology*, Vol. 2, No. 3, 1998, pp. 167–176.

[17]Cebeci, T., Chen, H. H., and Kaups, K., "Linear Stability Analysis of Three-Dimensional Flows with Surface Curvature: Effects of Sweep Angle and Reynolds Number," AIAA Paper 94-0827, 1994.

[18]Dewey, C. F., and Gross, J. F., "Exact Similar Solutions of the Laminar Boundary-Layer Equations," *Advances in Heat Transfer*, Vol. 4, 1967, pp. 317–446.

[19]Masson, C., Langlois, M., and Paraschivoiu, I., "A Linear Stability Analyser Suitable for Integration in Wing Performance Calculation Procedures," *ICAS Proceedings 1996 20th Congress of the International Council of the Aeronautical Sciences*, 1996, pp. 472–482.

[20]Langlois, M., Masson, C., and Paraschivoiu, I., "Fully-Three-Dimensional Transition Prediction on Swept Wings in the Transonic Regime," *Journal of Aircraft*, Vol. 35, No. 2, 1998, pp. 254–259.

[21]Langlois, M., Masson, C., Touchaud, S., and Paraschivoiu, I., "A Fast and Easy-to-Use Linear Stability Analyser for Wing Transition Predictions," AIAA Paper 97-2244, 1997.

[22]Langlois, M., "Prédiction de la transition sur des configurations tridimensionnelles en régime transsonique," Ph.D. Dissertation, Mechanical Engineering Dept., École Polytechnique de Montreal, Montreal, Feb. 2000.

[23]Archambaud, J. P., Payry, M. J., and Seraudie, A., "Étude expérimentale de la laminarité sur l'aile AS409 jusqu'à des nombres de Reynolds de l'ordre de 14 millions dans la soufflerie T2," TR 33/5006-19, ONERA, 1989.

[24]Boivin, S., "Étude des effets non parallèles sur la stabilité d'un écoulement tridimensionnel compressible," M.S. Thesis, Mechanical Engineering Dept., École Polytechnique de Montreal, Montreal, June 997.

[25]Schrauf, G., Perraud, J., Vitiello, D., and Lam, F., "A Comparison of Linear Stability Theories Using F100 Flight Tests," *Proceedings of the AIAA 15th Applied Aerodynamics Conference*, AIAA, Reston, VA, 1997, pp. 740–750.